SUPRAMOLECULAR CHEMISTRY
https://doi.org/10.1080/10610278.2019.1616089

Taylor & Francis
Taylor & Francis Group



# ZIF-8 degrades in cell media, serum, and some—but not all—common laboratory buffers

Michael A. Luzuriaga[a], Candace E. Benjamin[a], Michael W. Gaertner[a], Hamilton Lee[a], Fabian C. Herbert[a], Snipta Mallick[a] and Jeremiah J. Gassensmith[a,b]

[a]Department of Chemistry and Biochemistry; [b]Department of Biomedical Engineering, The University of Texas at Dallas, Richardson, TX, USA

**ABSTRACT**

Drug delivery using metal-organic frameworks (MOF) has elicited interest in their biocompatibility; however, few studies have been conducted on their stability in common buffers, cell media, and blood proteins. In particular, the use of ZIF-8, a MOF interconnected by Zn and methylimidazole, has been frequently employed. In this study, we tested single crystals of ZIF-8 with common laboratory buffers, cell media, and serum, and noted several issues. Buffers containing phosphate and bicarbonate alter the appearance and composition of ZIF-8; however, these buffers do not appear to cause cargo to leak out even when the ZIF-8 itself is displaced by phosphates. On the other hand, serum dissolves ZIF-8, causing premature cargo release. Our results show that ZIF-8 undergoes surface chemistry changes that may affect the interpretation of cellular uptake and cargo release data. On the other hand, it provides a rational explanation as to how ZIF-8 neatly dissolves in vivo.

**ARTICLE HISTORY**
Received 12 April 2019
Accepted 3 May 2019

**KEYWORDS**
Metal-organic frameworks; MOF; zeolitic imidazole frameworks; ZIFs; *in vitro*; *in vivo*; biocompatibility

## Introduction

Over the preceding two decades, metal-organic frameworks (MOFs) have been proposed for a number of industrial applications in catalysis (1, 2), and separations (3–5) and have more recently emerged as promising materials for biological sensing (6) and drug delivery (7–9). The applications for drug delivery have run from proposed systematic delivery of small molecules to the slow release of proteins *in vivo* (10, 11). A significant number of these MOFs in drug delivery have focused on two hydrolytically stable systems based on either zeolitic imidazole framework-8 (ZIF-8) (8, 9, 12), a coordination polymer composed of methyl-imidazole (HMIM) ligands bound to zinc that self-assembles into a zeolitic topological net, or zirconium-based systems, which use inorganic $Zr_6O_4(OH)_4$ polynuclear clusters as secondary building units typically linking benzodicarboxylic acid struts (13–15). While these systems are both well-known for their hydrolytic stability, biological milieu can be quite complex and, for *in vivo* or *in vitro* work, a number of aqueous buffered systems are used routinely. Of concern is that several of these buffers contain inorganic anions that can form kinetically trapped complexes with transition metals and MOF stability in buffers has been relatively unexplored (16). In particular, buffers based on phosphates and bicarbonate are fairly ubiquitous and these salts comprise a significant portion of cell media like Dulbecco's Modified Eagle's Medium (DME) as well as derivations of that media (DMEM, EMEM, etc.). Further, serum contains a substantial amount of albumin, which is a 66.5 kDa protein covered in solvent exposed thiols from externally facing cysteine residues (17). These residues are well known binders to metals and are a component of metal transport in blood (18–20).

Our interest in MOFs as potential drug delivery systems has focused on slow-release of large proteins for vaccine or therapeutic delivery by injecting the drug either subdermally or intramuscularly (21). Our approach has been to grow ZIF-8 non-specifically onto the surface of the proteins (22, 23), which not only thermally stabilizes the inlayed protein but also creates a 'slow release' mechanism for the protein to escape after implantation while protecting the protein from biological degradation by elevated temperatures or proteolytic enzymes (21). In this context, the slow dissolution of the ZIF is a critical component of drug release in that, over time, as the ZIF dissolves, it releases proteins that were 'biomimetically' integrated into the framework.

Because our MOF work frequently takes us both *in vivo* and *in vitro*, aqueous buffered solutions and cell media are frequently employed; thus, we sought to determine the stability of ZIF-8 in the most common

**CONTACT** Jeremiah J. Gassensmith gassensmith@utdallas.edu Department of Chemistry and Biochemistry, 800 West Campbell Road, Richardson, Texas 75080, United States

laboratory buffer systems as well as cell media, serum, and 'whole cell media' which is a mixture of cell media and serum. Our investigation revealed that neither phosphate nor carbonate-based buffers are innocent and induce almost immediate morphological changes as well as new and altered reflections in the PXRD pattern following exposure to these buffers. Beyond buffers, we found that serum 'burrows' holes into ZIF-8 crystals, the effects of which are imperceptible by PXRD, but cause cargo embedded in the crystalline matrix to leak out. In the context of controlled protein delivery via subdermal or intramuscular implantation, neither of these issues are problematic – in contrast, they help explain the protein release we have already observed (21). On the other hand, *in vitro* cell delivery and systemic delivery of small drugs may be complicated by these observations and the experimentalist should take care to interpret their results in light of these issues.

## Result and discussion

As described in the supporting information and Figure S1, we prepared ~1 µm sized ZIF-8 crystals by optimizing the final concentration of zinc acetate and HMIM solutions. Our ZIF-8 sample purity was confirmed by infrared spectroscopy (IR), scanning electron microscopy (SEM), and powder x-ray diffraction spectroscopy (PXRD). The crystals were not activated with organic solvent, but they were held under dynamic vacuum to remove excess wash water to dry them out for easier handling. These crystals were then weighed out into individual 15 mL falcon tubes and dispersed in different common lab buffers, which were buffered above pH 7.4. Additionally, we tested unbuffered 0.9% saline, which was measured to be mildly acidic from dissolved carbon dioxide. All samples were placed on a laboratory rotisserie to ensure proper mixing. Several buffers investigated had minimal effect on the apparent morphology of ZIF-8. Specifically, the 0.9% saline, 0.05 M Tris, and 0.025 M HEPES buffered solutions (Figure S3) yielded little apparent changes over 24 h by SEM while 1X PBS (phosphate buffered saline), 10X PBS, produced mild changes after several hours. On the other hand, within the first 10 mins, morphological changes—in some cases, significant ones—were apparent by SEM on ZIF-8 that had been placed in 0.1 M bicarbonate buffer, 0.1 M KP buffer, the cell media additive DMEM, bovine serum, and whole cell growth media, which is typically a combination of growth medium (DMEM in our case) with 10% serum. These morphological changes became even more obvious over time as can be seen in Figure 1 and continued until the end of our 24 h experiment (Figure S2). The changes observed when incubated with DMEM—a commonly used buffered cell growth medium—make sense, as these solutions contain 0.665 mM phosphate and 60.6 mM bicarbonate.

In addition to morphological analysis, all ZIF-8 samples were analysed by PXRD and EDX. Prior to this, solutions in their respective buffers and media were centrifuged at 4300 × *g* for 10 min at room temperature. The supernatant was pipetted off, its pH was measured, and free Zn content was analysed by ICP-MS (Table S1 and Table S2). The remaining pellet was washed three times with water and dried under vacuum for analysis. Changes to the bulk crystals were obvious by PXRD for all the phosphate and bicarbonate containing buffers and media—including DMEM. Because DMEM contains a significant amount of bicarbonate salts (60.6 mM), it is not surprising that incubation in DMEM and bicarbonate show similar reflections by PXRD—11.04°, 18.96°, and 23.92° 2$\theta$—in addition to the known ZIF-8 reflections (Figure 2(a)).

The 0.1 M potassium phosphate buffer (KP), on the other hand, completely eradicated the ZIF-8 replacing it with a different crystalline material altogether. Energy-dispersive X-ray (EDX) spectroscopy shows the resulting constituent crystals to likely be zinc and potassium phosphate salts with little HMIM remaining on the surface as noted by the lack of carbon or nitrogen (Figure 2(b) and S5). Considering the extensive changes with KP buffer, we were surprised that the PBS buffered solutions, which stands for 'phosphate buffered saline' showed markedly less changes in the PXRD spectra (Figure S4). While the standard laboratory 'recipe' for 1X PBS buffer uses an order of magnitude less phosphate, the 10X PBS buffer has the same phosphate concentration as 0.1 M KP buffer, yet 10X PBS buffers affects were clearly more mild over the same period of time as shown by PXRD (Figure S4). Tentatively, we ascribe this to the high NaCl concentration, which seems to suppress the release of free zinc into solution per inductively coupled mass spectrometry (ICP-MS) data presenting in Table S2.

Surprisingly, despite the apparent morphological changes to crystals left in bovine serum (Figure 1(e)), the PXRD for these samples remained largely unaffected, indicating that the crystallinity of the sample was not significantly altered (Figure 2(a)). The other buffers that had ZIF-8 were measured by PXRD and had no obvious changes in the spectrum, meaning that the buffers did not change the crystal (Figure S4). It is clear from ICP-MS data in Table S2 that serum was dissolving and solubilizing the Zn into solution, the most likely culprit being albumin.

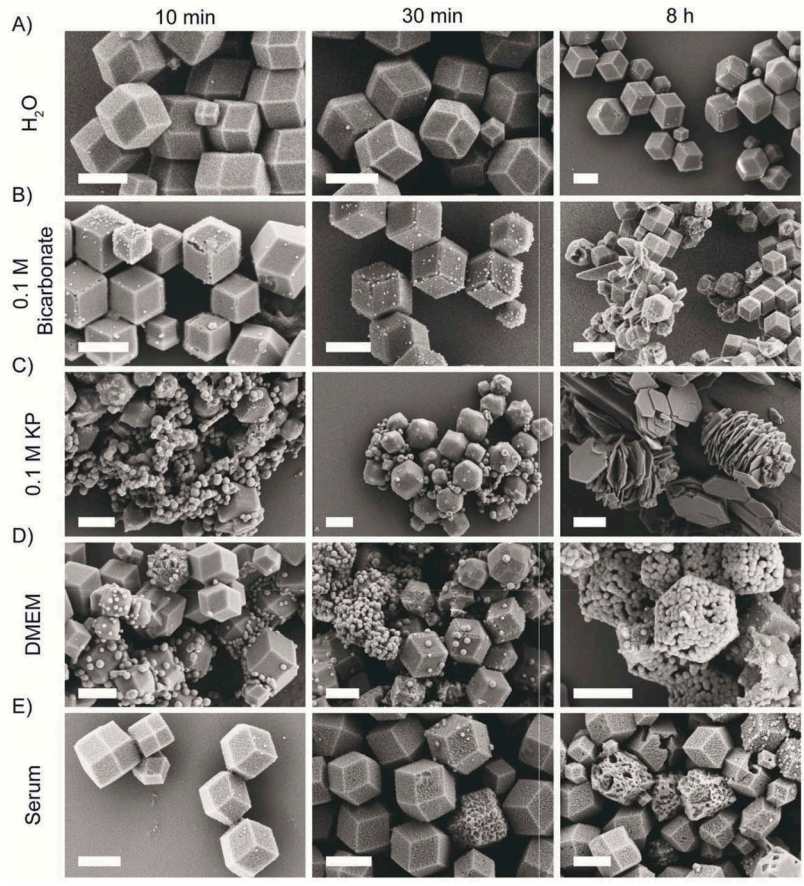


Figure 1. (Colour online) Time-resolved SEM micrographs of ZIF-8 incubated in (a) water pH 7.8, (b) 0.1 M bicarbonate buffer (pH 9.5), (c) 0.1 M KP buffer (pH 7.4), (d) DMEM (pH 7.6), and (e) serum (bovine serum, pH 7.9). At each time point, an aliquot of the ZIF-8 was taken and washed three times with water, dried, and imaged by SEM. (Scale bar: 1 μm.)

Finally, we wondered how these changes to the crystal composition and morphology would affect entrapped biomolecules with the assumption that some of the buffers that cause profound changes to morphology would lead to leaking. For the following study, green fluorescent protein (GFP)—a 27 kDa and barrel-shaped protein: 4.2 nm in length and 2.4 nm in diameter (24)—was biomimetically mineralized within ZIF-8 (Figure 3(a)) and the synthesized crystal was characterized by PXRD and FTIR (Figures S6 and S7). The crystal conditions were tuned such that the final crystal sizes were similar to the ones created for the preceding work as shown by DLS measurements (Figure S8) (25, 26). GFP@ZIF was individually incubated in the buffers mentioned above and ultrapure water and aqueous 0.5M EDTA – which completely dissolves the ZIF-8 – were used as controls. Separate samples were pelleted at 1, 4, and 24 h by centrifugation and fluorescence measurements of the supernatant were taken. Surprisingly, the only significant release of protein occurred in the serum, while in all other cases, only a very small release occurred close to the lower limit of detection. The exact amount of GFP released from the crystals can be found in Table S3 (Figures 3(b) and S9). The observed marginal release of GFP from ZIF-8 incubated in KP, DMEM and 0.1 M bicarbonate with the observed changes in morphology and crystal composition, suggests a double displacement reaction between salts in solution with the ZIF-8 that proceeds with one component—either the ZIF-8 or the salt—always remaining in the solid phase. In other words, even at very small scales, the salt exchange reaction appears to be completely heterogeneous. On the other hand, the GFP leaking from serum is attributable to the fact that, unlike the salts, the Zn is solubilized by serum proteins, thus the ZIF is literally dissolving into solution. This is corroborated by ICP-MS data that shows the supernatant obtained from serum had half the zinc concentration of the supernatant from an EDTA solution, which fully dissolves the ZIF-8. This dissolving of ZIF-8 by blood proteins causes approximately 40% of the GPF to be released within 24 h.

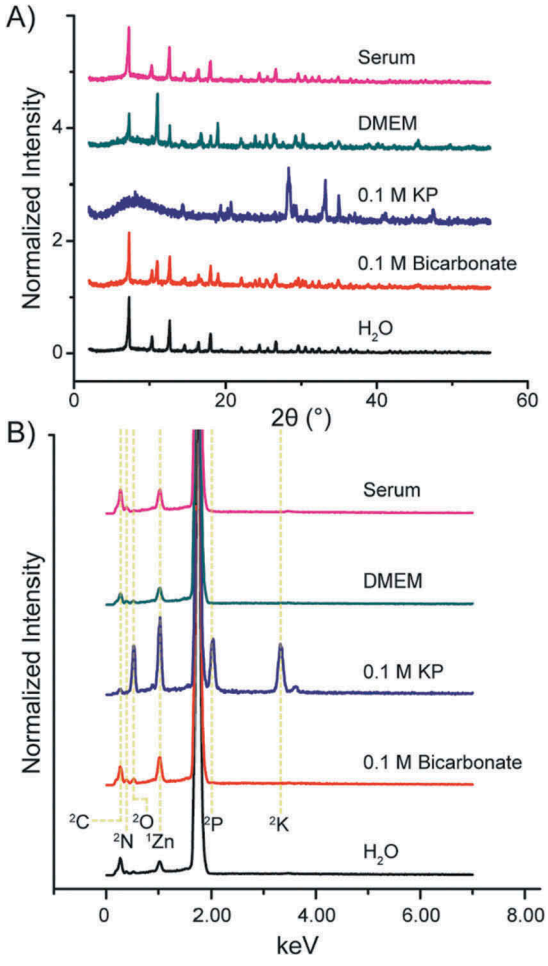


Figure 2. (Colour online) (a) PXRD and (b) EDX of ZIF-8 after 24 h of incubation with water, 0.1 M bicarbonate buffer, 0.1 M KP buffer, DMEM, and serum (superscript 1 are L shell electrons and superscript 2 are k shell electrons).

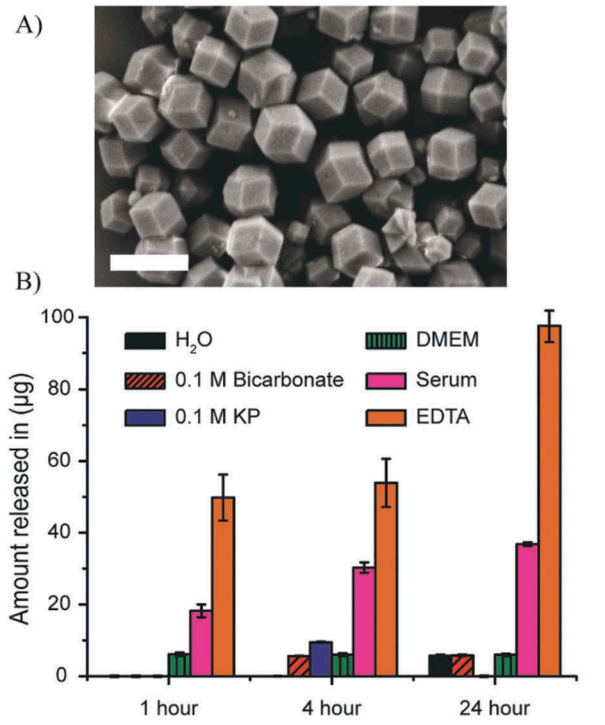


Figure 3. (Colour online) An SEM micrograph of (a) GFP@ZIF (scale bar: 1 µm) and time resolved fluorescence study showing (b) the release of GFP from ZIF after 1, 4, and 24 h incubation with water, 0.1 M bicarbonate buffer, 0.1 M KP buffer, DMEM, serum, and EDTA as a control.

## Conclusion

This study shows that ZIF-8 is not stable in certain buffers, even though they are all above pH 7, and that PXRD and electron microscopy studies are both needed together to fully demonstrate this. We have summarized our results to indicate the buffer and cell prep formulations that are 'compatible', 'should be used with caution', and 'not compatible' with ZIF-8 in Table 1. The stability seems to be a competition between the coordination bonds of zinc and 2-methylimidazole against strong inorganic and proteinaceous zinc binders, which include bicarbonate and phosphate and—surprisingly—serum proteins as well. That said, only serum seems to degrade ZIF-8 in such a way that allows significant quantities of GFP to escape. These experiments provide insight on the importance of buffer choice for *in vitro* and *in vivo* studies, storage, and drug delivery formulation.

Table 1. Buffer compatibility chart. ✓ compatible, ○ caution × not compatible.

| Buffer | No Surface Change | ZIF-8 Reflections | Not Leaky |
|---|---|---|---|
| $H_2O$ | ✓ | ✓ | ✓ |
| 0.9% saline | ✓ | ✓ | ✓ |
| 0.025 M HEPES | ○ | ✓ | ✓ |
| 0.05 M Tris | ○ | ✓ | ✓ |
| 0.1 M Bicarb | × | × | ○ |
| 1X PBS | ✓ | ✓ | ✓ |
| DMEM | × | ○ | ✓ |
| Serum | × | ✓ | × |
| Cell Media | × | ✓ | ○ |
| 10X PBS | × | ○ | ✓ |
| 0.1 M KP | × | × | ✓ |

Further, we are beginning to understand how ZIF-8 fully dissolves at physiological pH *in vivo* and it is clear that blood proteins, will play an important component.

We caution that these effects may change when using different sized proteins and we are not sure how translatable these results are to Zr-based MOFs; however, it is worth pointing out that, under mimicked physiological conditions, the Zr MOF UiO-66 seems to show analogous behaviour (27).

Finally, the changes in surface chemistry from the interactions with cell media clearly suggest that cells are likely not interacting with the surface of ZIF-8 – rather, they are interacting with a complicated surface of different formed salts and plasma proteins, this surface composition and morphology clearly depends upon incubation time and cell media choice. Consequently, we recommend experimental controls that include—as appropriate—cell media, buffers, and common plasma proteins to demonstrate morphological and chemical stability for projects that use MOFs for *in vitro* and *in vivo* applications.

## Author contributions

Primary manuscript writing and editing was done by M.A.L. and J.J.G. SEM, PXRD, and EDX was performed by M.A.L. ICP-MS studies was done by C.E.B. DLS was done by H.L. IR spectroscopy was done by F.H.C. GFP expression, purification, and characterization was done by C.E.B. and S.M. The synthesis of ZIF-8 and fluorescence release studies was done by M.A.L. and M.W.G. The buffers were made by M.W.G., M.A.L., and C.E.B.

## Disclosure statement

No potential conflict of interest was reported by the authors.

## Funding

J.J.G. would like to acknowledge the National Science Foundation, the [ACS-PRF 57627-DNI10], and Cancer Prevention and Research Institute of Texas [RP170752]; National Institutes of Health [1R21AI140462]; American Chemical Society Petroleum Research Fund [57627-DNI10]; Welch Foundation [AT-1989-20190330]; Division of Materials Research [DMR1654405].

## ORCID

Michael A. Luzuriaga http://orcid.org/0000-0001-6128-8800
Candace E. Benjamin http://orcid.org/0000-0002-9211-718X
Michael W. Gaertner http://orcid.org/0000-0003-2911-8160
Hamilton Lee http://orcid.org/0000-0003-2176-925X
Fabian C. Herbert http://orcid.org/0000-0002-0543-7151
Snipta Mallick http://orcid.org/0000-0001-8635-2354
Jeremiah J. Gassensmith http://orcid.org/0000-0001-6400-8106

## References

(1) Huxley, M.T.; Burgun, A.; Ghodrati, H.; Coghlan, C.J.; Lemieux, A.; Champness, N.R.; Huang, D.M.; Doonan, C. J.; Sumby, C.J. Protecting-Group-Free Site-Selective Reactions in a Metal–Organic Framework Reaction Vessel. *J. Am. Chem. Soc.* **2018**, *140*, 6416–6425. DOI: 10.1021/jacs.8b02896.

(2) Otake, K.-I.; Cui, Y.; Buru, C.T.; Li, Z.; Hupp, J.T.; Farha, O. K. Single-Atom-Based Vanadium Oxide Catalysts Supported on Metal–Organic Frameworks: Selective Alcohol Oxidation and Structure–Activity Relationship. *J. Am. Chem. Soc.* **2018**. doi:10.1021/jacs.8b05107.

(3) Hayashi, H.; Côté, A.P.; Furukawa, H.; O'Keeffe, M.; Yaghi, O.M. Zeolite A Imidazolate Frameworks. *Nat. Mater.* **2007**, *6*, 501–506. DOI: 10.1038/nmat1927.

(4) Li, L.; Yang, L.; Wang, J.; Zhang, Z.; Yang, Q.; Yang, Y.; Ren, Q.; Bao, Z. Highly Efficient Separation of Methane from Nitrogen on a Squarate-Based Metal-Organic Framework. *AIChE J.* **2018**, *64*, 3681–3689. DOI: 10.1002/aic.v64.10.

(5) Barter, M.; Hartley, J.; Yazigi, F.-J.; Marshall, R.J.; Forgan, R.S.; Porch, A.; Jones, M.O. Simultaneous Neutron Powder Diffraction and Microwave Dielectric Studies of Ammonia Absorption in Metal–Organic Framework Systems. *Phys. Chem. Chem. Phys.* **2018**, *20*, 10460–10469. DOI: 10.1039/c8cp00259b.

(6) Wang, Y.; Li, X.; Waterhouse, G.I.N.; Zhou, Y.; Yin, H.; Ai, S. Photoelectrochemical Biosensor for Protein Kinase A Detection Based on Carbon Microspheres, Peptide Functionalized Au-ZIF-8 and TiO2/g-C3N4. *Talanta*. **2019**, *196*, 197–203. DOI: 10.1016/j.talanta.2018.12.035.

(7) Zhuang, J.; Kuo, C.-H.; Chou, L.-Y.; Liu, D.-Y.; Weerapana, E.; Tsung, C.-K. Optimized Metal–Organic-Framework Nanospheres for Drug Delivery: Evaluation of Small-Molecule Encapsulation. *ACS Nano*. **2014**, *8*, 2812–2819. DOI: 10.1021/nn406590q.

(8) Zheng, H.; Zhang, Y.; Liu, L.; Wan, W.; Guo, P.; NyströM, A.M.; Zou, X. One-Pot Synthesis of Metal–Organic Frameworks with Encapsulated Target Molecules and Their Applications for Controlled Drug Delivery. *J. Am. Chem. Soc.* **2016**, *138*, 962–968. DOI: 10.1021/jacs.5b11720.

(9) Adhikari, C.; Das, A.; Chakraborty, A. Zeolitic Imidazole Framework (ZIF) Nanospheres for Easy Encapsulation and Controlled Release of an Anticancer Drug Doxorubicin under Different External Stimuli: A Way toward Smart Drug Delivery System. *Mol. Pharmaceutics*. **2015**, *12*, 3158–3166. DOI: 10.1021/acs.molpharmaceut.5b00043.

(10) Abánades Lázaro, I.; Haddad, S.; Rodrigo-Muñoz, J.M.; Marshall, R.J.; Sastre, B.; Del Pozo, V.; Fairen-Jimenez, D.; Forgan, R.S. Surface-Functionalization of Zr-Fumarate MOF for Selective Cytotoxicity and Immune System Compatibility in Nanoscale Drug Delivery. *ACS Appl. Mater. Interfaces*. **2018**, *10*, 31146–31157. DOI: 10.1021/acsami.8b11652.

(11) Welch, R.P.; Lee, H.; Luzuriaga, M.A.; Brohlin, O.R.; Gassensmith, J.J. Protein–Polymer Delivery: Chemistry from the Cold Chain to the Clinic.

*Bioconjugate Chem*. **2018**, *29*, 2867–2883. DOI: 10.1021/acs.bioconjchem.8b00483.

(12) Chen, -T.-T.; Yi, J.-T.; Zhao, -Y.-Y.; Chu, X. Biomineralized Metal-Organic Framework Nanoparticles Enable Intracellular Delivery and Endo-Lysosomal Release of Native Active Proteins. *J. Am. Chem. Soc*. **2018**, 140, 9912–9920. DOI: 10.1021/jacs.8b04457.

(13) Abánades Lázaro, I.; Abánades Lázaro, S.; Forgan, R.S. Enhancing Anticancer Cytotoxicity through Bimodal Drug Delivery from Ultrasmall Zr MOF Nanoparticles. *Chem. Commun*. **2018**, *54*, 2792–2795. DOI: 10.1039/C7CC09739E.

(14) Teplensky, M.H.; Fantham, M.; Li, P.; Wang, T.C.; Mehta, J.P.; Young, L.J.; Moghadam, P.Z.; Hupp, J.T.; Farha, O.K.; Kaminski, C.F.; Fairen-Jimenez, D. Temperature Treatment of Highly Porous Zirconium-Containing Metal–Organic Frameworks Extends Drug Delivery Release. *J. Am. Chem. Soc*. **2017**, *139*, 7522–7532. DOI: 10.1021/jacs.7b01451.

(15) Chen, Y.; Li, P.; Modica, J.A.; Drout, R.J.; Farha, O.K. Acid-Resistant Mesoporous Metal–Organic Framework toward Oral Insulin Delivery: Protein Encapsulation, Protection, and Release. *J. Am. Chem. Soc*. **2018**, *140*, 5678–5681. DOI: 10.1021/jacs.8b02089.

(16) Bellido, E.; Guillevic, M.; Hidalgo, T.; Santander-Ortega, M.J.; Serre, C.; Horcajada, P. Understanding the Colloidal Stability of the Mesoporous MIL-100(Fe) Nanoparticles in Physiological Media. *Langmuir*. **2014**, *30*, 5911–5920. DOI: 10.1021/la5012555.

(17) Oettl, K.; Stauber, R.E. Physiological and Pathological Changes in the Redox State of Human Serum Albumin Critically Influence Its Binding Properties. *Br. J. Pharmacol*. **2007**, *151*, 580–590. DOI: 10.1038/sj.bjp.0707251.

(18) Lu, J.; Stewart, A.J.; Sadler, P.J.; Pinheiro, T.J.; Blindauer, C.A. *Albumin as a Zinc Carrier: Properties of Its High-Affinity Zinc-Binding Site*. *Biochem. Soc. Trans*. 2008, 36, 1317–1321. DOI: 10.1042/BST0361317

(19) Cui, S.-F.; Peng, L.-P.; Zhang, H.-Z.; Rasheed, S.; Kumar, K. V.; Zhou, C.-H. Novel Hybrids of Metronidazole and Quinolones: Synthesis, Bioactive Evaluation, Cytotoxicity, Preliminary Antimicrobial Mechanism and Effect of Metal Ions on Their Transportation by Human Serum Albumin. *Eur. J. Med. Chem*. **2014**, *86*, 318–334. DOI: 10.1016/j.ejmech.2014.08.063.

(20) Stewart, A.J.; Blindauer, C.A.; Berezenko, S.; Sleep, D.; Sadler, P.J. Interdomain Zinc Site on Human Albumin. *Proc. Natl. Acad. Sci. U. S. A*. **2003**, *100*, 3701–3706. DOI: 10.1073/pnas.0436576100.

(21) Luzuriaga, M.A.; Welch, R.P.; Dharmarwardana, M.; Benjamin, C.E.; Li, S.; Shahrivarkevishahi, A.; Popal, S.; Tuong, L.H.; Creswell, C.T.; Gassensmith, J.J. Enhanced Stability and Controlled Delivery of MOF-Encapsulated Vaccines and Their Immunogenic Response in Vivo. *ACS Appl. Mater. Interfaces*. **2019**, *11*, 9740–9746. DOI: 10.1021/acsami.8b20504.

(22) Li, S.; Dharmarwardana, M.; Welch, R.P.; Ren, Y.; Thompson, C.M.; Smaldone, R.A.; Gassensmith, J.J. Template-Directed Synthesis of Porous and Protective Core–Shell Bionanoparticles. *Angew. Chem., Int. Ed*. **2016**, *55*, 10691–10696. DOI: 10.1002/anie.201604879.

(23) Li, S.; Dharmarwardana, M.; Welch, R.P.; Benjamin, C.E.; Shamir, A.M.; Nielsen, S.O.; Gassensmith, J.J. Investigation of Controlled Growth of Metal–Organic Frameworks on Anisotropic Virus Particles. *ACS Appl. Mater. Interfaces*. **2018**, *10*, 18161–18169. DOI: 10.1021/acsami.8b01369.

(24) Hink, M.A.; Griep, R.A.; Borst, J.W.; van Hoek, A.; Eppink, M.H.; Schots, A.; Visser, A.J. Structural Dynamics of Green Fluorescent Protein Alone and Fused with a Single Chain Fv Protein. *J. Biol. Chem*. **2000**, *275*, 17556–17560. DOI: 10.1074/jbc.M001348200.

(25) Wang, C.; Sun, H.; Luan, J.; Jiang, Q.; Tadepalli, S.; Morrissey, J.J.; Kharasch, E.D.; Singamaneni, S. Metal–Organic Framework Encapsulation for Biospecimen Preservation. *Chem. Mater*. **2018**, *30*, 1291–1300. DOI: 10.1021/acs.chemmater.7b04713.

(26) Liang, W.; Ricco, R.; Maddigan, N.K.; Dickinson, R.P.; Xu, H.; Li, Q.; Sumby, C.J.; Bell, S.G.; Falcaro, P.; Doonan, C.J. Control of Structure Topology and Spatial Distribution of Biomacromolecules in Protein@ZIF-8 Biocomposites. *Chem. Mater*. **2018**, *30*, 1069–1077. DOI: 10.1021/acs.chemmater.7b04977.

(27) Abánades Lázaro, I.; Haddad, S.; Sacca, S.; Orellana-Tavra, C.; Fairen-Jimenez, D.; Forgan, R.S. Selective Surface PEGylation of UiO-66 Nanoparticles for Enhanced Stability, Cell Uptake, and pH-Responsive Drug Delivery. *Chem*. **2017**, *2*, 561–578. DOI: 10.1016/j.chempr.2017.02.005.